

# Robust Tracking Performance and Disturbance Rejection for a Class of Nonlinear Systems Using Disturbance Observers

Ahmed H. El-Shaer and Masayoshi Tomizuka

**Abstract**— This paper is concerned with disturbance rejection performance in single-input single-output (SISO) nonlinear systems described by uncertain linear dynamics and bounded nonlinearities. After transforming the nonlinear terms into an equivalent bounded disturbance at the output of a linear system, a disturbance observer (DOB) is added to achieve robust disturbance rejection. The DOB design is formulated as Luenberger observer state estimation for an augmented system which contains at least one eigenvalue at the origin. The synthesis of a (sub)optimal DOB is carried out by solving multi-objective  $H_\infty$  sensitivity optimization. The design approach is applied to an inverted pendulum with actuator backlash.

## I. INTRODUCTION

This paper is concerned with robust tracking performance and disturbance rejection for a class of single-input single-output (SISO) nonlinear systems. The system dynamics is comprised of a linear part subject to norm-bounded uncertainty [5], and a vector-valued bounded nonlinearity which is not known exactly. Given an internally stabilizing controller which renders the nominal linear dynamics exponentially stable, the nonlinearities can be represented as a bounded disturbance  $d(t) \in \mathbb{R}$  at the output of a linear system. A disturbance observer (DOB) is then introduced into the feedback system to eliminate the effect of  $d(t)$  in the presence of the linear plant uncertainty.

The main objective in this paper is to extend linear DOB-based disturbance rejection, using the  $H_\infty$  robust control framework [6], to feedback systems comprised of the uncertain nonlinear plant dynamics given by (1). This will be accomplished without the need for special change of coordinates i.e. local diffeomorphism [13] ch. 13. In particular, the approach presented below applies directly to both matched and mismatched disturbance/uncertainty inputs. This overcomes restrictive matched conditions which need to be present in existing disturbance rejection strategies for many nonlinear systems, see [2][10] and the references therein.

DOBs are successfully used in many industrial applications including robotics, hard disk drives high-precision servo systems and machine drive tools, see [3] [17][22]. Moreover, in [19] DOBs are effectively used to suppress the effect of a class of nonlinearities which can be decomposed into a linear part and a bounded nonlinearity. In DOB-based control, an inner loop having a unity-DC gain low pass filter

$Q(s)$ , is added into the main feedback system to estimate exogenous disturbances and cancel them subsequently [8].

The robust DOB design presented in this paper relies on the equivalence of the DOB structure in Fig. 1b and that of a classic Luenberger observer state estimation of an augmented linear system with internal model for the disturbance dynamics [12]. Under mild assumptions it is shown that such equivalence indeed exists if the internal model has at least an eigenvalue at the origin [17][8]. Thus, once the Luenberger observer gain  $L$  is obtained,  $Q(s)$  is evaluated as a transfer function parameterized by the gain  $L$ , i.e.  $Q(s, L)$ . This approach offers many advantages over conventional methods [22]: (i) the design of DOBs is systematically embedded into the more general framework of robust state estimation for uncertain [9] and nonlinear systems [10], (ii) the design of the outer controller and the inner DOB can be carried out completely separately, (iii) structure constraints associated with  $Q(s)$  filter (e.g. the DC constraint  $Q(0) = 0$ ) are readily satisfied in the new design, (iv) additional frequency shaping can be transparently introduced into the DOB by incorporating appropriate disturbance modes in the internal model dynamics. Thus, the DOB filter  $Q(s)$  can be designed with more flexibility in regards to its order, bandwidth and roll-off rate. Hence, disturbance rejection performance is greatly enhanced and robustness of the overall system is achieved.

The DOB synthesis is formulated as a constrained  $H_\infty$  sensitivity optimization which can be efficiently solved for a local (sub)optimal observer gain in a number of ways including semi-definite programming [8], nonlinear programming [15][14] and non-smooth  $H_\infty$  synthesis [1] [11]. Finally, the design approach is applied to a nonlinear inverted pendulum with input backlash nonlinearity. Simulation results indicate that DOB-based control achieves robust tracking and disturbance rejection of the closed loop system.

## II. PROBLEM STATEMENT

This paper is concerned with the SISO nonlinear system

$$\begin{aligned}\dot{x} &= Ax + Bu + g(x, u) \\ y &= Cx,\end{aligned}\tag{1}$$

where  $x(t) \in \mathbb{R}^n$ ,  $u(t), y(t) \in \mathbb{R}$ , and  $g: \mathbb{R}^n \times \mathbb{R} \rightarrow \mathbb{R}^n$  is vector-valued nonlinearity collecting nonlinear terms in the plant and actuator. It is assumed that the functional form of  $g(\cdot, \cdot)$  is not exactly known, however the map  $t \mapsto g(x(t), u(t)) \in L_\infty^n$ , that is

$$\|g\|_{L_\infty} := \max_{1 \leq i \leq n} \sup_{\chi(t) \in \mathbb{R}^{n+1}} \sup_{t \geq 0} |g_i(x(t), u(t))| \leq m_g < \infty, \tag{2}$$

Ahmed H. El-Shaer is R & D control scientist at LineStream Technologies, Cleveland OH, USA (ahshaer@gmail.com).

Masayoshi Tomizuka is with the Department of Mechanical Engineering, University of California at Berkeley, CA, USA (tomizuka@me.berkeley.edu).

where  $\chi(t) := [x(t)^T u(t)^T]^T$ . The assumption (2) is satisfied by many nonlinearities arising in dynamical systems such as flexible-joint robots [21], classes of chaotic systems [20] as well as a number of play-stop hysteresis operators [9]. Also,  $g(\cdot, \cdot)$  can represent an unknown norm-bounded perturbation acting on a linearized system, see [13] ch. 9. Furthermore, the transfer function  $P(s) = C(sI - A)^{-1}B$  satisfies the multiplicative uncertainty

$$P(s) = P_n(s)(1 + \Delta(s)), \Delta(s) \text{ stable}, \|\Delta\|_\infty \leq 1, \quad (3)$$

where  $\|\cdot\|_\infty$  is the  $H_\infty$  norm [5][6], and  $P_n(s) = C_p(sI - A_p)^{-1}B_p$  is the nominal transfer function. Hence, the nominal nonlinear system is

$$\begin{aligned} \dot{x}_p &= A_p x_p + B_p u + g(x_p, u) \\ y_p &= C_p x_p. \end{aligned} \quad (4)$$

The following assumptions are made

- (A1) The nominal plant  $P_n(s)$  is minimum phase,
- (A2) The pair  $(A_p, C_p)$  is detectable.

Let  $K(s)$  (4) be an internally stabilizing controller designed *a priori* to achieve good tracking performance for  $P_n(s)$

$$\begin{aligned} \dot{x}_k &= A_k x_k + B_k e \\ u &= C_k x_k + D_k e \end{aligned} \quad (5)$$

where  $x_k(t) \in \mathbb{R}^{n_k}$ ,  $e(t) = y_{ref}(t) - y_p(t)$  is the nominal tracking error, and  $y_{ref}(t) \in \mathbb{R}$  is a bounded reference input. From (4) and (5), the output  $y_p$  of the nominal closed loop system is given by

$$y_p(t) = \underbrace{C_{cl} \left[ e^{A_{cl}t} x_{cl}(0) + \int_0^t e^{A_{cl}\psi} \begin{bmatrix} B_p D_k \\ B_k C_k \end{bmatrix} y_{ref}(t - \psi) d\psi \right]}_{y_{nom}(t)} + \underbrace{C_{cl} \int_0^t e^{A_{cl}\psi} g_{cl}(x_{cl})(t - \psi) d\psi}_{y_{pert}(t)}, \quad (6)$$

where  $x_{cl} = \begin{bmatrix} x_p \\ x_k \end{bmatrix}$ ,  $A_{cl} = \begin{bmatrix} A_p - B_p D_k C_p & B_p C_k \\ -B_k C_p & A_k \end{bmatrix}$ ,  $C_{cl} = [C_p \ 0]$  and  $g_{cl}(x_{cl}) = \begin{bmatrix} g(x_p, C_k x_k + D_k e) \\ 0 \end{bmatrix}(t)$ . In (6),  $y_{nom}$  denotes the response of the nominal linear dynamics and  $y_{pert}$  is a perturbation term accounting for  $g(\cdot, \cdot)$ . Since  $A_{cl}$  is Hurwitz, it follows that

$$\begin{aligned} d(t) &:= y_{pert}(t) = C_{cl} \int_0^t e^{A_{cl}\psi} g_{cl}(x_{cl})(t - \psi) d\psi \\ \Rightarrow \|d(t)\| &\leq k \|C_{cl}\|_\infty \int_0^t e^{-\alpha\theta} \|g(x_{cl})(t - \theta)\| d\theta \leq \frac{k \|C_{cl}\|_\infty m_g}{\alpha}, \end{aligned} \quad (7)$$

where  $k > 0$  and  $\alpha > 0$  such that  $\|e^{A_{cl}t}\| \leq k e^{-\alpha t}$  [4] p. 59.

Thus,  $d$  (7) is a norm-bounded exogenous disturbance at the output  $y_p$ . In the presence of  $\Delta(s)$ , exponential stability of the underlying linear closed loop dynamics (i.e. (1) with  $g(\cdot, \cdot) \equiv 0$ ), is sufficient for  $d(t)$  to be uniformly bounded, which will be established below using the small gain theorem. This motivates the use of a disturbance observer (DOB) to achieve robust closed loop tracking performance by rejecting potentially degrading effects of  $d(t)$  so that the closed loop recovers nominal linear behavior for all  $\Delta(s)$  satisfying (3). Clearly, the construction in this section includes both *matched* and *mismatched* nonlinearities.

### III. DISTURBANCE OBSERVERS

#### A. Overview

As shown in Fig. 1, the DOB introduces an inner loop into the feedback system where  $Q(s)$  is a *stable unity DC gain low pass filter with desired bandwidth*, and is considered the design parameter. DOB-based control is studied in more details in [17] and in El-Shaer et.al. [8]. In Fig. 1a,  $d$  captures the effect of the nonlinearities  $g(\cdot, \cdot)$  in the plant/actuator dynamics. The primary objective of the DOB is to produce an estimate  $\hat{w}$  and *feed it back* to the nominal control input  $u$  to cancel the effect of  $d$ . It is important to note that  $\hat{w}$  represents the equivalent estimate of  $d$  reflected at the plant's control input. From Fig. 1a

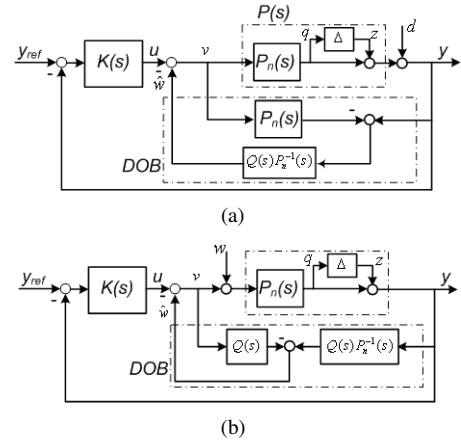


Fig. 1. DOB-based closed loop system: (a) The exogenous disturbance  $d$  at the output, (b) equivalent DOB structure with exogenous disturbance  $w$  at the input

$$\begin{aligned} \hat{w} &= Q(s) P_n^{-1}(s) (y - P_n(s) v) \\ \Rightarrow \hat{w} &= Q(s) P_n^{-1}(s) y - Q(s) v. \end{aligned} \quad (8)$$

Thus, the DOB scheme in Fig. 1a is equivalent to that in Fig. 1b, with the latter regarded as rejection of an exogenous disturbance  $w$  at the input of  $P(s)$ . It is noted that  $Q(s) P_n^{-1}$  is stable by assumption (A1). It is shown in the sequel that the DOB structure in Fig. 1b is equivalent to a Luenberger observer of an augmented dynamical system. This renders the design of optimal DOB more systematic and overcomes structural constraints associated the filter  $Q(s)$ . Hence, the DOB configuration in Fig. 1b is used in the analysis hereafter.

#### B. Robust Disturbance Rejection

From Fig. 1b, assuming that  $P_n(s) = P(s)$ , the output  $y = y_p$  is given by

$$y = \frac{P_n(s) K(s) y_{ref} + P_n(s) (1 - Q(s)) w}{1 + P_n(s) K(s)}. \quad (9)$$

From Fig. 1b, the following closed loop sensitivity functions are defined

$$S(s) = \frac{P_n(s) (1 - Q(s))}{1 + P_n(s) K(s)}, T(s) = \frac{P_n(s) K(s) + Q(s)}{1 + P_n(s) K(s)}, \quad (10)$$

where  $S(s) = -G_{w \rightarrow e}(s)$ , and  $T(s) = -G_{z \rightarrow q}(s)$  where  $z$  and  $q$  are interconnection variables of the nominal closed

loop system and the uncertainty  $\Delta(s)$ . Eq. (10) indicates that further reduction in  $S(s)$  is achieved by having  $Q(s) = 1$  over a desired frequency band. Consequently, for a stable  $Q(s)$ , the sensitivity function  $T(s)$  is exponentially stable. Thus, given  $W_u(s)$  a stable weighting function such that  $|\Delta(j\omega)| \leq |W_u(j\omega)| \forall \omega$  and  $\Delta(s)$ , the *small gain* condition [5][6]

$$\|W_u T\|_\infty < 1 \quad (11)$$

guarantees that the closed loop in Fig. 1a is (internally) exponentially stable  $\forall \Delta(s)$  in (3). Therefore  $d(t)$  in Fig. 1a is  $L_\infty$ -bounded signal, hence also  $\hat{w} \in L_\infty$ .

It is also noted that  $G_{w \rightarrow \hat{w}}(s) = Q(s)$ . Thus, given a stable weighting function  $W_p(s)$ , then

$$\|W_p(1-Q)\|_\infty \leq \gamma \implies \|W_p(w - \hat{w})\|_{L_2} \leq \gamma \|w\|_{L_2}, \quad (12)$$

where  $\gamma > 0$  is a given performance bound and  $w - \hat{w}$  is the disturbance estimation error (Fig. 1b). Hence, (11) and (12) guarantee robust disturbance rejection. Also  $\|W_p(1-Q)\|_\infty \leq \gamma$  sets a lower bound on the cut-off frequency of the high pass filter  $1-Q(s)$ . Thus,  $W_p(s)$  can be selected to set desired bandwidth for  $Q(s)$ . The conditions (11) and (12) will be used in the sequel to formulate a multi-objective  $H_\infty$  optimization for the DOB synthesis.

### C. Q Filter Design

The filter  $Q(s)$  is typically given by [3][17][8][22]

$$Q(s) = \left(1 + \sum_{k=1}^{m-\rho} a_k (\tau s)^k\right) \left(1 + \sum_{k=1}^m a_k (\tau s)^k\right)^{-1}, \quad (13)$$

where  $m > 0$  is the order of  $Q(s)$  and  $\rho \leq m$  is its relative degree. The design trade-off of  $Q(s)$  is to choose  $\{a_k\}_{k=1}^m \geq 0$  such that its cut-off frequency  $\omega_c \approx 1/\tau$  is large enough for better disturbance rejection. However, a direct synthesis of  $Q(s)$  given by (13) is subject to

- (Q1) *Relative degree*:  $\rho$  must be greater than or equal the relative degree of  $P_n(s)$  to make  $Q(s)P_n^{-1}(s)$  realizable,
- (Q2) *Unity DC gain*:  $Q(0) = 1$  imposes that  $\rho$  and  $\{a_k\}_{k=1}^m$  are not independent of each other [22],
- (Q3) *Robust stability* given by (11).

These conditions complicate the synthesis of an optimal  $Q(s)$ . Thus, an alternative design method is desired where the structure constraints ((Q1) and (Q2) above) are implicitly satisfied to ease the complexity of the synthesis process.

### D. Internal Model-based Luenberger Observer

In this section, robust disturbance estimation is formulated as the design of a Luenberger observer for an augmented system with an internal model of the disturbance. It is shown that the DOB-based disturbance estimation given in Fig. 1b is equivalent to that based on the Luenberger observer. Consequently,  $Q(s)$  satisfying (Q1), (Q2) and (Q3) is parameterized by the Luenberger observer gain which can be systematically designed via a multi-objective  $H_\infty$  sensitivity optimization.

The analysis below is concerned with a general exogenous disturbance  $w(t)$  which is not necessarily the same as the

effect of the nonlinearity  $d(t)$  (7) reflected at the input of the plant as was done in Fig. 1b, see *Remark 2* below. Suppose the disturbance  $w(t)$  is generated by the exo-system [12]

$$\begin{aligned} \dot{x}_w &= A_w x_w, & x_w(t_0) &= x_{w0} \\ w &= C_w x_w, \end{aligned} \quad (14)$$

where  $x_w(t) \in \mathbb{R}^{n_w}$ . The state space representation in (14) is assumed to satisfy

- (A3) The pair  $(A_w, C_w)$  is detectable,
- (A4) The eigenvalues of  $A_w$  don't coincide with the zeros of the plant  $P_n(s)$  (i.e. the disturbance state  $x_w$  is observable from the output  $y_p$ ).

Let  $\tilde{x} = [x_p^T x_w^T]^T$ , the augmented system, comprised of the nominal plant and the exo-system, is given by (see Fig. 2)

$$\begin{aligned} \dot{\tilde{x}} &= \tilde{A}\tilde{x} + \tilde{B}v, & \tilde{y} &= \tilde{C}\tilde{x} \\ \tilde{A} &= \begin{bmatrix} A_p & B_p C_w \\ 0 & A_w \end{bmatrix}, & \tilde{B} &= \begin{bmatrix} B_p \\ 0 \end{bmatrix}, & \tilde{C} &= [C_p \ 0] \end{aligned} \quad (15)$$

Given assumptions (A2), (A3) and (A4), it can be shown that

$$\text{rank} \left( \begin{bmatrix} \lambda I - \tilde{A} \\ \tilde{C} \end{bmatrix} \right) = \begin{bmatrix} \lambda I - A_p & -B_p C_w \\ 0 & \lambda I - A_w \\ C_p & 0 \end{bmatrix} = n_p + n_w \quad (16)$$

for all eigenvalues  $\lambda \in \mathbb{C}$  of  $\tilde{A}$  [8][21]. From the PBH observability rank condition [6] p. 82, it follows that the augmented system (15) is detectable. Hence, there exists  $L \in \mathbb{R}^{n_p+n_w}$  such that

$$\dot{\hat{x}} = (\tilde{A} - L\tilde{C})\hat{x} + \begin{bmatrix} \tilde{B} & L \end{bmatrix} \begin{bmatrix} v \\ y_p \end{bmatrix} \quad (17)$$

is an asymptotically stable state observer for the augmented system (15). Moreover, using the coordinate transformation  $T = \begin{bmatrix} I & 0 & 0 & 0 \\ 0 & I & 0 & 0 \\ 0 & 0 & I & 0 \\ 0 & 0 & 0 & I \end{bmatrix} (\in \mathbb{R}^{2n_p+n_k+n_w})$ , the eigenvalues of the overall closed loop system, comprised of  $P_n(s)$ ,  $K(s)$  and the Luenberger observer (17), can be decomposed as follows

$$\begin{aligned} \det(\lambda I - T^{-1} \begin{bmatrix} A_p - B_p D_k C_p & B_p C_k & 0 & -B_p C_w \\ -B_k C_p & A_k & 0 & 0 \\ L_1 C_p - B_p D_k C_p & B_p C_k & A_p - L_1 C_p & 0 \\ L_2 C_p & 0 & -L_2 C_p & A_w \end{bmatrix} T) \\ = \det(\lambda I - A_{cl}) \det(\lambda I - (\tilde{A} - L\tilde{C})), \end{aligned} \quad (18)$$

where  $A_{cl}$  is given in (6),  $\tilde{A} - L\tilde{C} = \begin{bmatrix} A_p - L_1 C_p & B_p C_w \\ -L_2 C_p & A_w \end{bmatrix}$  and  $L = [L_1^T L_2^T]^T$  with  $L_1 \in \mathbb{R}^{n_p}$  and  $L_2 \in \mathbb{R}^{n_w}$ . Thus, closed loop exponential stability is achieved if and only if each of  $A_{cl}$  and  $\tilde{A} - L\tilde{C}$  is Hurwitz. This clearly allows  $K(s)$  to be designed separately of the state estimator.

### E. Equivalence to the DOB

The 2 cases shown in Fig. 2, are now considered for disturbance estimation

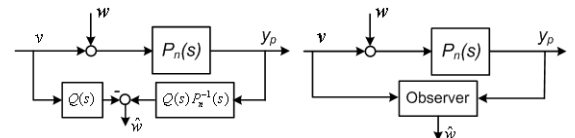


Fig. 2. Disturbance estimation: DOB (left), observer based (right)

1. *Observer-based*: from (17) and Fig. 2, the estimate  $\hat{w}$  is given by

$$\begin{aligned} \hat{w} &= -G_1(s) v + G_2(s) y_p \\ \begin{bmatrix} \frac{G_1(s)}{G_2(s)} \end{bmatrix} &= \tilde{C}_w (sI - (\tilde{A} - L\tilde{C}))^{-1} \begin{bmatrix} -\tilde{B} \\ L \end{bmatrix}, \\ \tilde{C}_w &= \begin{bmatrix} 0 & C_w \end{bmatrix} \end{aligned} \quad (19)$$

2. *DOB-based*: from (8), the estimate  $\hat{w}$  is given by

$$\hat{w} = -Q(s) v + Q(s) P_n^{-1}(s) y_p. \quad (20)$$

The equivalence between the *observer-based* and the *DOB-based* estimates is stated next.

**Theorem 1:** Suppose that assumptions (A2), (A3) and (A4) are satisfied, and that  $A_w$  has at least one of its eigenvalues at the origin. Then the expressions in (19) and (20) for  $\hat{w}$  are equivalent; that is,  $Q(s) = G_1(s)$  and  $Q(s) P_n^{-1}(s) = G_2(s)$ . In particular,  $Q(0) = G_1(0) = 1$ .

**Proof:** Details in [17] pp. 543–546  $\square$ .

In particular,  $G_1(s)$  is a *low-pass filter with unity DC gain*, and  $Q(s) P_n^{-1}(s) = G_2(s)$  is indeed realizable; both (Q1) and (Q2) are satisfied. Once  $L$  is obtained,  $Q(s)$  is evaluated using  $G_1(s)$  in (19). From Theorem 1 it follows that a Luenberger observer with sufficiently large bandwidth allows the DOB-based estimate  $\hat{w}$  (20) to asymptotically track any  $w$  given by (14); that is  $\lim_{t \rightarrow \infty} (w(t) - \hat{w}(t)) = 0$ . Together with (12) and (11), robust asymptotic disturbance estimation and rejection are indeed achieved.

**Remark 1:** Some advantages of this approach are: (i) the structure constraints (Q1) and (Q2) are satisfied, (ii) internal stability of the nominal closed loop system is guaranteed by virtue of (18), and (iii) a wide variety of exogenous disturbances can be transparently accommodated into this design by incorporating their signal models in  $A_w$  (see (21)).

**Remark 2:** It must be emphasized that  $d(t)$  resulting from the nonlinearity  $g(\cdot, \cdot)$  (7), *is not* generated by (14) which serves as a fictitious augmented state to ensure that  $Q(s)$  satisfies (Q1) and (Q2). This enables DOB-based controllers to reject signals not having well defined spectral content. Disturbances other than  $d(t)$  (7) can be treated by expressing  $w(t)$  in (14) as

$$\begin{aligned} w(t) &= A_1 w_1(t) + A_2 w_2(t) \\ W_1(s) &= \frac{1}{s^{a_{w1}}}, W_2(s) = \frac{n_{w2}(s)}{d_{w2}(s)}, \end{aligned} \quad (21)$$

where  $w_1(t)$  ensures that  $A_w$  has at least one eigenvalue at the origin. Different choices of  $d_{w2}(s)$  allows  $w_2(t)$  to model a wide variety of exogenous disturbances. Moreover, the amplitudes  $A_1$  and  $A_2$  are scaling factors to reduce measurement noise amplification, also when  $A_2 \equiv 0$  the so-called proportional-integral (PI) Luenberger observer is recovered, see [21].

#### IV. SYNTHESIS OPTIMIZATION

From (11), (12) and (19), an optimal  $Q(s)$  can be synthesized from the following constrained  $H_\infty$  sensitivity optimization

$$\min_{L \in \mathbb{R}^{n_p + n_w}} \|W_p(s) (1 - Q(s, L))\|_\infty \quad (22a)$$

$$\text{subject to: } \|W_u(s) T(s, L)\|_\infty < 1, \quad (22b)$$

$$\|W_p(s) (1 - Q(s, L))\|_\infty \leq \gamma, \quad (22c)$$

$$\max_i \operatorname{Re}\{\lambda_i\{\tilde{A} - L\tilde{C}\}\} \leq -\sigma_S \quad (22d)$$

where  $Q(s, L) = G_1(s)$ , and  $T(s, L)$  is given by (10),  $\gamma > 0$  and  $\sigma_S > 0$  are given performance and stability bounds, respectively. The inequality (22d), ensures that the estimation error dynamics  $\tilde{A} - L\tilde{C}$  is *fast* and *well damped* with  $-\sigma_S$  guaranteed decay rate. For practical purposes, (22) is usually restricted to problem-specific finite frequency intervals which reflect desired performance. The expressions (22) involve the non-smooth  $H_\infty$ -norm, and are non-convex in  $L$ . In El-Shaer et. al. [8][9], the synthesis (22) is expressed as the weighted sensitivity optimization:

$$\min_L \gamma \quad \text{subject to: } \left\| \begin{bmatrix} W_u T \\ W_p (1 - Q) \end{bmatrix} \right\|_\infty \leq \gamma, \gamma < 1,$$

which is then turned into rank-constrained semi-definite program (SDP) [6] p. 231, for a static output feedback (sub)optimal  $L$ . However, the solution obtained might be too conservative since both robust stability (22b) and robust performance (22c) are expressed by a single Lyapunov SDP variable, see [8] for details. Alternatively, parametric optimization over  $L$  using nonlinear programming (NLP) gives freedom to maintain individual performance constraint bounds, at the expense of non-smooth objective and constraint functions.

Given an initial observer gain  $L_0$ , a local (sub)optimal  $L$  of (22) can be obtained using subgradient-based non-smooth  $H_\infty$  synthesis of fixed-structure controllers presented in [1]. Currently, this algorithm solves sensitivity minimization without additional eigenvalue-placement constraints, i.e. unconstrained single or multiple sensitivity problems [11]. However, for the more general setting (e.g. (22)), finite difference approximation of the gradients allows available powerful interior-point NLP algorithms to handle multi-objective  $H_\infty$ -synthesis constraints, see [15] ch. 19 and [14]<sup>1</sup>.

#### V. SIMULATION EXAMPLE

The rotation dynamics of a fixed-based inverted pendulum about the vertically upright equilibrium position (i.e.  $\theta = 0$ ,  $\dot{\theta} = 0$ ) is

$$\begin{aligned} m l^2 \ddot{\theta} + b \dot{\theta} + k \theta &= m g l \sin(\theta) + T_{in}(u) + T_{dist}; \\ m &= 0.25[\text{kg}], l = 0.5[\text{m}], b = 0.001[\text{N.m.sec}], \\ k &= 0.1[\text{N.m/rad}], g = 9.81[\text{m/sec}^2] \end{aligned} \quad (23)$$

In (23),  $T_{in} = N(u)$  [N.m] is the input torque,  $u$  is the control signal,  $N(\cdot)$  is backlash nonlinearity in the drive shaft and  $T_{dist}$  [N.m] represents disturbance torques.

The presence of backlash is known to cause limit cycle oscillations in closed loop systems [16]. The graph of a non-symmetric backlash nonlinearity is displayed in Fig. 3, where the slopes  $m_1$ ,  $m_2$  and  $K_N$  are finite, and the dead-band width is given by  $\Delta_1 - \Delta_2$ , see [16][7][18]. An exact analytic form of  $N(\cdot)$  might be too complicated and is not needed for robust DOB design. In fact, the output of  $N(u)(t)$  can be

<sup>1</sup>Due to space limitations, details of the algorithms mentioned are omitted, see the references cited.

written as  $N(u)(t) = K_N u(t) + \eta(t)$  [18][19], where  $\eta(t)$  is a nonlinearity such that

$$\|\eta\|_\infty = \sup_{t \geq 0} |\eta(t)| \leq \max \left\{ \sup_{u(t) \in \mathbb{R}} (m_+(u) - K_N u), \sup_{u(t) \in \mathbb{R}} (K_N u - m_-(u)) \right\}. \quad (24)$$

In (24)  $m_+(\cdot)$  and  $m_-(\cdot)$  are piecewise continuous curves such that  $m_-(u(t)) \leq N(u)(t) \leq m_+(u(t))$ ,  $\forall t \geq 0, u \in L_\infty$ . Given  $K_N$ , the choices  $m_+(u) := K_N u + n_u$  and  $m_-(u) := K_N u - n_u$ , establish that the smallest  $n_u$  intercepting the  $N(\cdot)$ -axis is a bound on  $\|\eta\|_\infty$ , see Fig. 3. Thus,  $\eta$  is indeed norm bounded.

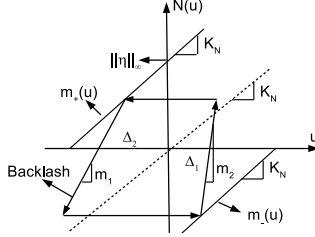


Fig. 3. Graph of the backlash  $N(\cdot)$

The state space representation of (23) is given by

$$\dot{x} = \begin{bmatrix} 0 & 1 \\ -\frac{k}{m l^2} & -\frac{b}{m l^2} \end{bmatrix} x + \begin{bmatrix} 0 \\ \frac{K_N}{m l^2} \end{bmatrix} u + \begin{bmatrix} 0 \\ \frac{g \sin(x_1)}{l} + \frac{\eta(t)}{m l^2} \end{bmatrix} + \begin{bmatrix} 0 \\ \frac{1}{m l^2} \end{bmatrix} T_{dist} \quad (25)$$

$$y = [1 \ 0] x$$

which is the same as (1) with the additional term  $T_{dist}$ . The slope  $K_N$  is assumed to be given by  $K_N = \bar{K}_N + r_K \delta_K$ ;  $\bar{K}_N = 1$ ,  $r_K = 0.75$  and  $|\delta_K| \leq 1$ . From (23)  $P(s) = \frac{K_N}{m l^2 s^2 + b s + k}$  and  $P_n(s) = \frac{\bar{K}_N}{m l^2 s^2 + b s + k}$ , which yields  $W_u(j\omega) = \frac{|P(j\omega) - P_n(j\omega)|}{|P_n(j\omega)|} \leq r_K$ . The outer controller, designed based on  $P_n(s)$ , is chosen as a simple lead compensator

$$K(s) = 2.5 \frac{5s + 1}{0.25s + 1} \quad (26)$$

to achieve good tracking up to  $1.5 \text{ Hz}$ .

Let  $T_{dist}$  represent structure vibration modeled as lightly damped sinusoid at  $\omega_w$ . The total disturbance (21) is given by

$$w(t) = A_1 \eta(t) + A_2 T_{dist}, \quad (27)$$

where  $A_1 = 100, A_2 = 500$ . Choosing  $W_1(s) = \frac{1}{s}$  and  $W_2(s) = \frac{\omega_w^2}{s^2 + 2\zeta\omega_w s + \omega_w^2}$ ;  $\zeta = 0.002$ ,  $\omega_w = 5(2\pi) [\text{rad/sec}]$ , the exo-system (14) is given by

$$A_w = \begin{bmatrix} 0 & 0 & 0 \\ 0 & 1 & 0 \\ 0 & -\omega_w^2 & -2\zeta\omega_w \end{bmatrix}, C_w = [A_1 \ A_2 \ 0]. \quad (28)$$

It is easily verified that the conditions in Theorem 1 are satisfied.  $W_p(s)$  is chosen as

$$W_p(s) = 0.5 \frac{s + 2(2\pi)}{s + 0.5} \frac{s^2 + 2(0.8\zeta)\omega_w s + \omega_w^2}{s^2 + 2(1.5\zeta)\omega_w s + \omega_w^2}, \quad (29)$$

which has a resonant mode at  $\omega_w$  and specifies at least  $8 \text{ Hz}$  cut-off frequency for  $Q(s)$ . Eigenvalue placement for  $\tilde{A}$  at  $\{-8, -12, -18, -24, -34\}$  yields  $L_0 = [154.62, 5.99, 0.893, -4.648, -245.985]^T$ .

## A. Optimization Results

For  $\sigma_s = 8$  and  $\gamma = 2$ , the NLP (22) is specialized to

$$\min_{L \in \mathbb{R}^5} \max_{\omega \in (2\pi) \times [0.1, 8]} |W_p(j\omega)(1 - Q(j\omega, L))|, \quad (30)$$

subject to: (22b), (22c), (22d),

which confines the objective (22a) to the frequency range  $\omega \in (2\pi) \times [0.1, 8] [\text{rad/sec}]$ . The NLP (30) is solved using the interior point solver within the `fmincon` command in the Optimization Toolbox, Matlab Version 7.14 (R2012a), which implements a trust region-based sequential quadratic programming (SQP), see [14]<sup>2</sup>. Convergence takes place after 60 iterations to  $L = [1561.3, 15.174, 121.18, 144.91, -163.2]$  with objective function value  $\max_{\omega \in (2\pi) \times [0.1, 8]} |W_p(j\omega)(1 - Q(j\omega, L))| = 0.36$ .

For comparison, Table 1 shows solution results for (22) using the iterative SDP algorithm [8] and the non-smooth synthesis [1] which is implemented by `hinfstruct` in the Robust Control Toolbox, Matlab (R2012a) [11]. From Table 1, robust stability (i.e.  $\|W_u T\|_\infty < 1$ ) is satisfied only by the NLP-based solution (i.e. with `fmincon`), which will be used below for closed loop simulation. From (19) the DOB filter for the NLP-based synthesis is

$$Q(s) = \frac{1.353 \times 10^6 s^2 - 1.136 \times 10^6 s + 1.914 \times 10^8}{s^5 + 242.9 s^4 + 2.6 \times 10^4 s^3 + 1.596 \times 10^6 s^2 + 2.353 \times 10^7 s + 1.914 \times 10^8}, \quad (31)$$

which is stable unity-DC gain with cut-off frequency at  $13 \text{ Hz}$ . From Table 1,  $Q(s)$  in (31) satisfies the robust performance bound (22c)  $\|W_p(1 - Q)\|_\infty = 1.48 < \gamma = 2$  and the robust stability  $\|W_u T\|_\infty = 0.986 < 1$  (22b), see also Fig. 4.

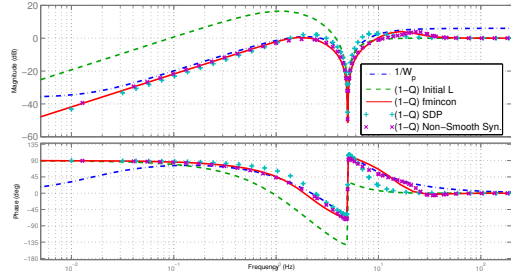


Fig. 4. Bode plots of  $1/W_p(s)$  (dash-dot),  $1 - Q(s)$ ; initial  $L$  (dash), NLP  $L$  (solid), SDP  $L$  (+), Non-smooth synthesis  $L$  (x)

## B. Simulation Results

All simulations are carried out in Simulink Version 7.9 (R2012a) for the closed loop comprised of the nonlinear system (23), the outer controller  $K(s)$  (26) and DOB inner loop with  $Q(s)$  (31). In both cases below, tracking error  $e = y_{ref} - y$  is obtained for  $y_{ref}(t) = \frac{\pi}{3} \sin(2\pi f t)$ ;  $f = \frac{3}{4} \text{ Hz}$ , in the presence of the disturbance torque  $T_{dist}(t) = \sin(\omega_w t)$ ;  $\omega_w = 5(2\pi) [\text{rad/sec}]$ .

1) *Case I: Inverted Pendulum without Backlash*: In this case  $T(u) = u$  in (23). The closed loop response is shown in Figs. 5 and 6. The rms values of the tracking error are 0.0482 and 0.0744 for the closed loop with and without the DOB, respectively.

<sup>2</sup>Central difference is chosen to approximate gradients with relative perturbation  $1 \times 10^{-6}$ , and the BFGS for Hessian updates. The command `norm` is used to compute the  $H_\infty$  norm.

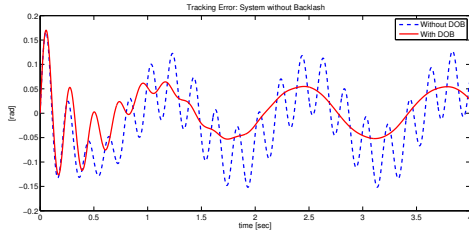


Fig. 5. No backlash:  $e = y_{ref} - y$ ; with DOB (solid), w/o DOB (dash)

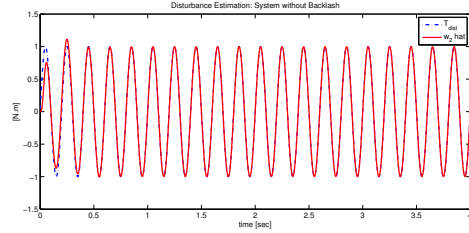


Fig. 6. No backlash:  $T_{dist}$  (dash-dot) and  $\hat{w}_2$  (solid)

2) *Case II: Inverted Pendulum with Backlash*: A symmetric backlash with dead-band width of 0.3 (i.e.  $\Delta_1 = -\Delta_2 = 0.15$ ) and slope  $K_N = 0.75$  (i.e. 0.25 perturbation in the nominal value) is used. The closed loop response is given in Figs. 7 and 8. The rms values of the tracking error  $e$  are 0.0483 and 0.0754 for the closed loop with and without the DOB, respectively.

In both cases  $\hat{w}_2$  is obtained in two steps; first the closed loop is simulated without  $T_{dist}$  to get  $\hat{w} = \hat{w}_1$ , then simulated with  $T_{dist}$  to get the overall estimate  $\hat{w}$ . Then from (21)  $\hat{w}_2 = \hat{w} - \hat{w}_1$ . Clearly, robust closed loop tracking performance is achieved with the DOB which provides disturbance estimation and rejection in the presence of  $T_{dist}$ .

## VI. CONCLUSIONS

A DOB-based control approach is presented to for disturbance rejection and tracking performance in a class of uncertain SISO nonlinear systems. Robustness analysis is studied within the  $H_\infty$  framework. Synthesis strategies using

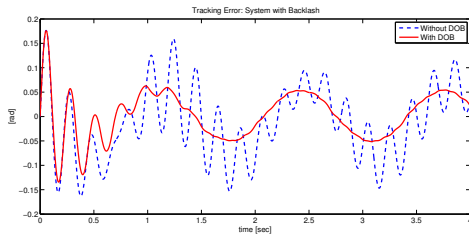


Fig. 7. With backlash:  $e = y_{ref} - y$ ; with DOB (solid), w/o DOB (dash)

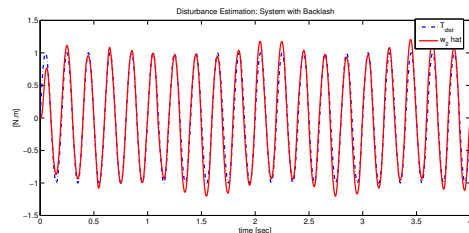


Fig. 8. With backlash:  $T_{dist}$  (dash-dot) and  $\hat{w}_2$  (solid)

	NLP (fmincon)	SDP	Non-smooth $H_\infty$ (hinfstruct)
$\ W_u T\ _\infty$	0.986	1.41	1.32
$\ W_p (1 - Q)\ _\infty$	1.48	1.45	1.14
$\max \text{Re}\{\lambda_i\{A - LC\}\}$	-8.4	-7.78	-11.96

TABLE I  
OPTIMIZATION RESULTS

NLP, SDP and non-smooth optimization were discussed. Simulation results of an inverted pendulum show that closed loop robust tracking performance is indeed achieved using the DOB.

## REFERENCES

- [1] P. Apkarian and D. Noll, Nonsmooth  $H_\infty$  Synthesis. *IEEE Trans. on Automatic Control*, vol. 51, no. 1, 2006.
- [2] J. Back and H. Shim, Adding Robustness to Nominal Output-Feedback Controllers for Uncertain Nonlinear Systems: a Nonlinear Version of Disturbance Observer. *Automatica*, vol. 44, 2008.
- [3] R. Bickel and M. Tomizuka, Passivity-Based Versus Disturbance Observer Based Robot Control: Equivalence and Stability. *ASME Journal of Dynamic Systems, Meas. and Control*, vol. 121, pp. 41-47, 1999.
- [4] C. Desoer and M. Vidyasagar. *Feedback Systems: Input-Output Properties*. Academic Press, 1975.
- [5] J. Doyle, B. Francis, and A. Tannenbaum. *Feedback Control Theory*. Macmillan Publishing Co., 1990.
- [6] G. E. Dullerud and F. Paganini. *A Course in Robust Control Theory*. Springer-Verlag, New York, 2000.
- [7] R. V. Dwivedula and P. R. Pagillar, Effect of Compliance and Backlash on the Output Speed of a Mechanical Transmission System. *ASME Journal of Dynamic Systems, Meas. and Control*, vol. 134, 2012.
- [8] A. H. El-Shaer and T. Zhang, On Robust Disturbance Observer Design Using Semi-Definite Programming, *Proc. of the Dynamic Systems Control Conference*, Arlington, VA 2011.
- [9] A. H. El-Shaer, M. Al Janaideh, P. Krejčí and M. Tomizuka, Robust Performance Enhancement Using Disturbance Observers for Hysteresis Compensation Based on Generalized Prandtl-Ishlinskii Model, *Proc. of the American Control Conference*, Montreal, QC 2012.
- [10] L. B. Freidovich and H. K. Khalil, Performance Recovery of Feedback-Linearization-Based Designs. *IEEE Trans. on Automatic Control*, vol. 53, no. 10, 2008.
- [11] P. Gahinet and P. Apkarian, Structured  $H_\infty$  Synthesis in MATLAB. *Proc. of the 18th IFAC World Congress*, Milano, Italy, 2011.
- [12] C. D. Johnson, Accommodation of External Disturbances in Linear Regulator and Servomechanism Problems. *IEEE Trans. of Automatic Control*, vol. 16, no. 6, 1971.
- [13] H. K. Khalil. *Nonlinear Systems*. Prentice Hall, 2002.
- [14] Matlab Optimization Toolbox, User's Guide R2012b. The MathWorks Inc.
- [15] J. Nocedal and S. Wright. *Numerical Optimization*. Springer, 2006.
- [16] M. Nordin and P. -O. Gutman, Controlling Mechanical Systems with Backlash – A Survey. *Automatica*, vol. 38, 2002.
- [17] E. Schrijver and J. V. Dijk, Disturbance Observers for Rigid Mechanical Systems: Equivalence, Stability and Design. *ASME Journal of Dynamic Systems, Meas. and Control*, vol. 124, pp. 539-548, 2002.
- [18] R. R. Selmic and F. L. Lewis, Backlash compensation in nonlinear systems using dynamic inversion by neural networks. *Proc. of the IEEE Intl. Conference on Control Applications*, Kohala Coast, HI, 1999.
- [19] S. Shahruz, Performance Enhancement of a Class of Nonlinear Systems by Disturbance Observers. *IEEE/ASME Trans. on Mechatronics*, vol. 5, no. 3, pp. 319-323, 2000.
- [20] S. Shahruz, Suppression of Effects of Nonlinearities by Disturbance Observers. *Proc. of the American Control Conference*, Boston, Massachusetts, 2004.
- [21] D. Söffker, Tie-Jun Yu and P. C. Müller, State Estimation of Dynamical Systems with Nonlinearities by Using Proportional-Integral Observer, *International Journal of Systems Science*, vol. 26, 1571-1582, 1995.
- [22] T. Umeno, T. Kaneko and Y. Hori. Robust Servosystem Design with Two Degrees of Freedom and its Application to Novel Motion Control of Robot Manipulators, *IEEE Trans. on Industrial Elec.*, vol. 40, No. 5, 1993.